PHYSICAL REVIEW B **80**, 020404(R) (2009)

Fermi-liquid state and enhanced electron correlations in the iron pnictide $CaFe_4As_3$

Liang L. Zhao,[1] Tanghong Yi,[2] James C. Fettinger,[2] Susan M. Kauzlarich,[2] and E. Morosan[1]
[1]*Department of Physics and Astronomy, Rice University, Houston, Texas 77005, USA*
[2]*Department of Chemistry, University of California at Davis, One Shields Avenue, Davis, California 95616, USA*
(Received 20 March 2009; revised manuscript received 30 June 2009; published 24 July 2009)

The recently discovered $CaFe_4As_3$ system displays low-temperature Fermi-liquid behavior, with enhanced electron-electron correlations. At high temperatures, the magnetic susceptibility shows Curie-Weiss behavior, with a large temperature-independent contribution. Antiferromagnetic ordering is observed below $T_N=(88.0\pm1.0)$ K, possibly via a spin density wave transition. A remarkably sharp drop in resistivity occurs below $T_2=(26.4\pm1.0)$ K, correlated with a similarly abrupt increase in the susceptibility but no visible feature in the specific heat. The electronic specific-heat coefficient γ at low temperatures is close to 0.02 J mol_{Fe}^{-1} K^{-2}, but a higher value for $\gamma\sim0.08$ J mol_{Fe}^{-1} K^{-2} can be inferred from a linear Cp/T vs T^2 just above T_2. The Kadowaki-Woods ratio $A/\gamma^2=55*10^{-5}$ $\mu\Omega$ cm mol^2 K^2 mJ^{-2} is nearly two orders of magnitude larger than that of heavy fermions.

DOI: 10.1103/PhysRevB.80.020404 PACS number(s): 75.30.Fv, 72.15.−v, 65.40.Ba

Many advances in science in general, and in condensed matter in particular, have been brought about by the discovery of new materials. The most recent example is the high-temperature iron-oxypnictide superconductors,[1] a case of accidental incorporation of oxygen in a rare earth iron pnictide ternary via tin flux. After the original discovery of superconductivity in La(O/F)FeAs, the past year has seen a revival of the interest in superconductivity, fueled by the discovery of additional classes of homologous superconductors based on $BaFe_2As_2$,[2,3] FeSe,[4] and LiFeAs,[5,6] and an increase in T_c to new records (over 50 K) for noncuprate materials. Here we present the structural and physical properties of another Fe-As compound, $CaFe_4As_3$, also reported by Todorov *et al.*[7] Despite lack of superconductivity down to 1.8 K, this compound shows complex electronic and magnetic properties.

$CaFe_4As_3$ is a framework structure composed of shared Fe-As tetrahedra, with Ca atoms (blue/large spheres, Fig. 1) sitting in channels defined by these shared tetrahedra. Two phase transitions are observed in this material, an antiferromagnetic (AFM) ordering below $T_N\approx88.0$ K, likely associated with a spin density wave (SDW) transition, and a lower transition around $T_2\approx26.4$ K. Fermi-liquid behavior with enhanced electron correlations is observed below this lower transition. As a result, the Kadowaki-Woods (KW) ratio is nearly two orders of magnitude larger than the corresponding value for heavy fermions, with a correspondingly enhanced Wilson ratio (R).

Single crystals of $CaFe_4As_3$ have been synthesized using tin flux, starting from a composition Ca:Fe:As:Sn $=1:4:3:40$. The constituent elements were placed in evacuated silica tubes, slowly heated up to 1100 °C, and followed by slow cooling to 600 °C. After the tin flux was decanted, well-formed thin rods were obtained, typically about 1 mm^2 in cross section and up to 8 mm long. Anisotropic magnetization measurements were performed using the Reciprocating Sample Option (RSO) of the Quantum Design Magnetic Property Measurement System. Specific-heat measurements were performed in a QD Physical Property Measurement System, using an adiabatic relaxation technique. Given the rodlike geometry of the sample, the ac resistivity measurements ($i=1$ mA, $f=17.77$ Hz) were done for current along the rod axis. The structure of $CaFe_4As_3$ was determined by single-crystal x-ray diffraction, and no detectable flux incorporation was observed. Needle shape crystals were cut to size ($\sim0.22\times0.11\times0.08$ mm^3) and placed in a nitrogen stream. Diffraction data were acquired using a Bruker SMART 1000 charge coupled device (CCD) diffractometer utilizing a graphite-monochromatic Mo $K\alpha$ radiation ($\lambda=0.71073$ Å) at $T=90(2)$ K and the SMART software package. SAINT was employed for data frame integrations. SADABS was used to correct the data for Lorentz and polarization effects and to apply a numerical absorption correction. XPREP was used to identify the space group and to create the data files. The structure was determined by direct methods with SHELXS and refined with SHELXL.[8]

Above 90 K, $CaFe_4As_3$ is orthorhombic (space group *Pnma*) with lattice parameters $a=11.8840(7)$ Å, $b=3.7342(2)$ Å, and $c=11.5857(7)$ Å. There are four crystallographic sites for Fe (small spheres, Fig. 1) and several close Fe-Fe distances, between 2.5952(6) and 2.8629(4) Å. The Fe1-Fe3 atoms are fourfold coordinated with As (me-

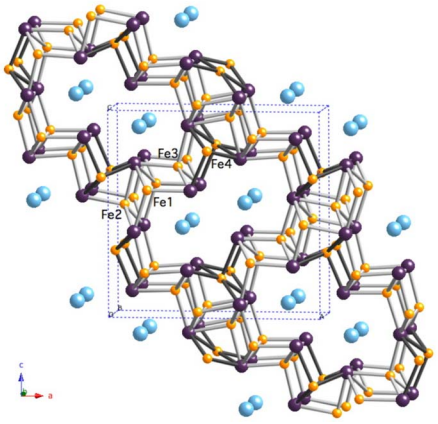

FIG. 1. (Color online) *ac*-plane view of the $CaFe_4As_3$ structure, with the Ca, Fe, and As represented by blue (large), orange (small), and purple (medium) spheres, respectively. Fourfold coordinated Fe and As atoms form buckled sheets (gray bonds) similar to the Fe-As planes in Fe-pnictide superconductors; these fold back into each other around the fivefold coordinated Fe4 atoms.

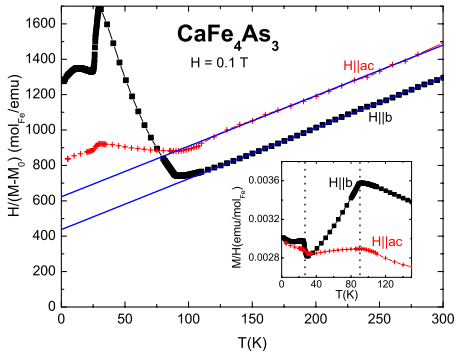

FIG. 2. (Color online) Anisotropic inverse magnetic susceptibility $1/\Delta\chi(T)(\Delta\chi(T)=\chi(T)-\chi_0)$ for $H=0.1$ T, and $H\|ac$ (crosses) and $H\|b$ (full squares). The straight lines represent the high-temperature fits to the Curie-Weiss law after the constant χ_0 has been taken into account. Inset: total low-temperature anisotropic $\chi(T)$ showing a sharp decrease below $T_N=87.0$ K and an upturn around the low-T transition $T_2=26.4$ K.

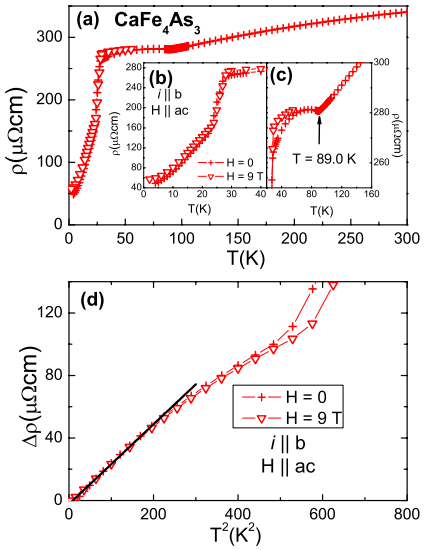

FIG. 3. (Color online) Resistivity of $CaFe_4As_3$ for $i\|b$, and $H=0$ (crosses) and $H=9$ T (triangles) $(H\perp i)$. Details around the (b) T_2 and (c) T_N transitions. (d) Low-temperature $\Delta\rho=\rho-\rho_0$ vs T^2, with the residual resistivity $\rho_0\approx 42$ $\mu\Omega$ cm as determined from (b); straight line is a fit to $\Delta\rho=\rho-\rho_0=AT^2$, which gives $A=0.25$ $\mu\Omega$ cm K^{-2}.

dium spheres) (gray lines, Fig. 1), giving rise to buckled Fe-As sheets similar to the Fe-pnictide planes in the new superconductors. These sheets fold back into each other around the fivefold coordinated Fe4 atoms, forming channels along the b axis, with the Ca atoms (large spheres, Fig. 1) sitting in these channels. Additional crystallographic information can be found in the supplementary information.[9]

The anisotropic inverse susceptibility $1/\Delta\chi(T)=H/(M(T)-M_0)$ is shown in Fig. 2 for an applied magnetic field $H=0.1$ T. At high temperatures ($T>130$ K) the susceptibility (Fig. 2) can be fit to a Curie-Weiss law $\chi(T)=M(T)/H=\chi_0+C/(T-\theta)$ after a temperature-independent contribution χ_0 has been accounted for. Larger $\chi(T)$ values are observed for $H\|b$ (black squares, inset Fig. 2) than for $H\|ac$ (red crosses, inset Fig. 2). The χ_0 values sum up the core diamagnetic, Pauli and Landau contributions, and are determined from the data fits to be $2.23*10^{-3}$ and $1.76*10^{-3}$ emu mol_{Fe}^{-1} for $H\|b$ and $H\|ac$, respectively. Such large χ_0 values strongly suggest enhanced Pauli paramagnetism [since the core diamagnetism is typically on the order of $10^{-6}-10^{-5}$ emu mol^{-1} (Ref. 10) and $\chi_{Landau}\approx -1/3\chi_{Pauli}$]. As a result of the observed anisotropy associated with crystal field effects, a reduced effective moment $\mu_{eff}=1.66\mu_B$/Fe is determined for both field orientations, in agreement with the values calculated by Todorov *et al.*[7] This is much smaller than the theoretical values expected for either $Fe^{2+}(4.9-6.7\mu_B/\text{Fe})$ or $Fe^{3+}(5.9\mu_B/\text{Fe})$.[11] Although $CaFe_4As_3$ is not superconducting above 1.8 K, nor does it have the layered Fe-As structure ubiquitous in the new Fe superconductors, the structure is comprised of Fe-As buckled sheets, similar to the infinite planes in the latter compounds. The reduced moment per Fe ion is also reminiscent of the Fe superconductors: $0.4-0.8\mu_B$/Fe for the *R*OFeAs compounds[12] and close to $0.87\mu_B$/Fe for $BaFe_2As_2$.[13] One more notable similarity is a AFM-like transition, which occurs in $CaFe_4As_3$ around $T_N=88.0$ K, very close to the previously reported ordering temperature[7] and the SDW transition temperature observed in single crystals of $BaFe_2As_2$.[14]

Given the resistivity behavior around T_N (Fig. 3), it is plausible that the ordering in $CaFe_4As_3$ may also be associated with a SDW transition: The high-temperature resistivity is linearly decreasing with T, typical of a metal. Thus for a simple AFM metal, one would expect a drop in the resistivity below T_N, associated with loss of spin-disorder scattering. However, the resistivity of $CaFe_4As_3$ has a weak minimum at $T_N\approx 89.0$ K [Fig. 3(c)], followed by a broad maximum at lower temperatures, similar to the behavior observed in Cr, a typical SDW system.[15] The AFM transition is also consistent with the $H=0$ specific heat data (Fig. 4), which shows a peak centered around 87 K. An identical $C_p(T)$ measurement was recorded in an applied magnetic field $H=9$ T (not shown for clarity).

A more complex phase transition is observed upon further lowering the temperature. After a decrease in $\chi(T)$ below T_N, a sharp increase occurs below 26.4 K (inset, Fig. 2). This is associated with a similarly abrupt drop in resistivity [Fig. 3(b)], followed by a much stronger decrease at lower temperatures compared to the high-T regime. However this transition cannot be detected in the specific heat data (Fig. 4) so a careful analysis of the low-temperature properties of $CaFe_4As_3$ is imperative.

At least two scenarios can be considered in explaining the transition below 26.4 K: by analogy with Cr,[15] a spin-flip transition is possible in the SDW state, between a transversely polarized state (where the spin direction **S** and the wave vector **q** are orthogonal) and a longitudinally polarized state (where **S** and **q** are parallel). Another possibility would be a weak structural distortion. This may be associated with the enhancement of the density of states at the Fermi surface, which in turn increases the Pauli susceptibility while correspondingly reducing the electrical resistivity. The lack of any signature of the 26.4 K transition in the specific heat data seems to render more credibility to the spin-flip hypothesis. However, as is shown below, the low-temperature properties

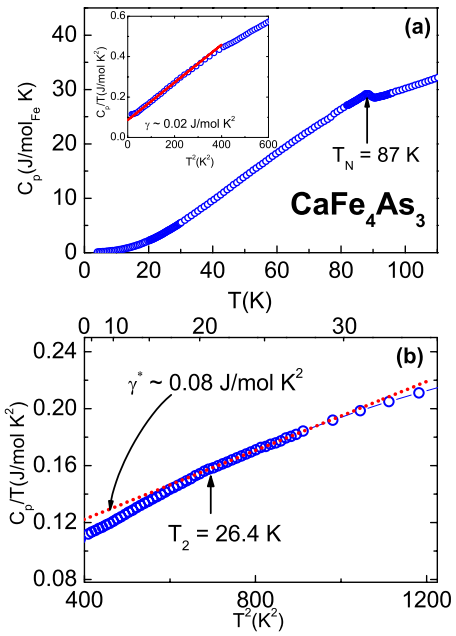

FIG. 4. (Color online) (a) $H=0$ specific heat data, with the AFM transition at $T_N=87$ K marked by the vertical arrow. Inset: low-temperature region, together with the expected linear fit (straight line) to $C_p/T=\gamma+\beta T^2$, which yields $\gamma=0.02$ J/(mol K^2). (b) C_p/T vs T^2 around $T_2=26.4$ K and a dotted line showing a linear fit above T_2 with a new $\gamma^*=0.08$ J/(mol K^2).

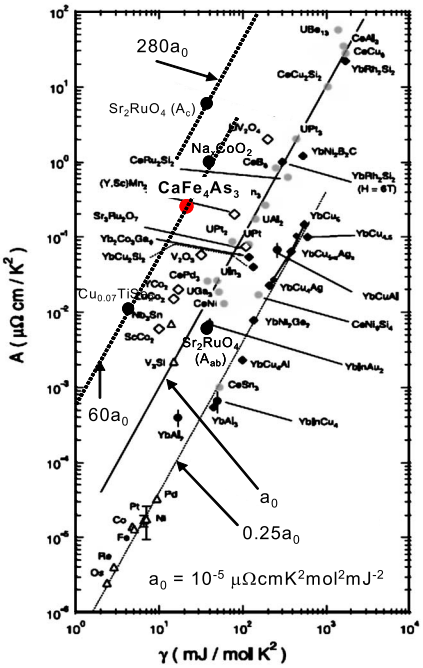

FIG. 5. (Color online) Kadowaki-Woods plot A vs γ [reproduced from (Ref. 21)], with $CaFe_4As_3$ shown as large red symbol. $CaFe_4As_3$ has similar KW ratio to $Na_{0.07}CoO_2$ (Ref. 23) and $Cu_{0.07}TiSe_2$ (Ref. 24), smaller only than that for Sr_2RuO_4 (for $i\|c$) (Ref. 22).

of $CaFe_4As_3$ are dominated by strong electron-electron coupling, which may conceal a phonon-driven feature in the specific heat at low temperatures.

Based on the susceptibility measurements, the large χ_0 contributions already point to enhanced electron interactions compared to a free-electron system. Moreover, below $T<20$ K, the specific heat data can be fit to $C_p/T=\gamma+\beta T^2$ [inset, Fig. 4(a)], which gives the electronic and lattice specific heat coefficients $\gamma=0.02$ J/(mol$_{Fe}$ K^2) and $\beta=0.23*10^{-3}$ J/(mol$_{Fe}$ K^4), respectively. The corresponding Debye temperature is approximately $\theta_D=260$ K. γ is comparable to the respective value for $BaFe_2As_2$ (Ref. 14) but much larger than that reported for LaOFeAs (Ref. 16) and $CaFe_2As_2$ (Ref. 17) and, more importantly, significantly enhanced compared to the free-electron model. An estimate of the Wilson ratio $R=4\chi_0/(3\gamma)(\pi k_B/\mu_{eff})^2$ (Ref. 18) gives a remarkably large value $R=8-10$ for the two applied field directions. Given that the magnetic susceptibility does not saturate at 2 K (Fig. 2, inset) $\chi_0=1.76-2.23*10^{-3}$ emu/mol is a better estimate of the Pauli susceptibility than $\chi(T=2\ \text{K})=3*10^{-3}$ emu/mol, but the two are very close to each other. For a noninteracting Fermi liquid, R is expected to be close to 1, and it has been shown to be closer to 2 for strongly correlated electron systems.[19] Julian *et al.*[20] showed that higher R values occur in nearly ferromagnetic (FM) metals. Density functional theory calculations[7] on $CaFe_4As_3$ seem to support the hypothesis of FM coupling at low temperatures, which may also explain the upturn in $\chi(T)$ at the lowest temperatures in our data (inset, Fig. 2). Another plausible explanation for the large Wilson ratio can be drawn from the low-temperature transition. If indeed the transition below $T<26.4$ K has a structural component, this would affect the electron-phonon interactions and thus γ but would not change χ_0. In this case the high Wilson ratio would be an artifact due to the fact that the γ and χ_0 values correspond to the low- and high-temperature states, respectively. Although no phase transition can be detected in the specific heat measurement, C_p/T vs T^2 [Fig. 4(b)] appears to change to a linear region with lower slope and larger γ for almost a 10 K interval above T_2: $\gamma^*\simeq 0.08$ J/(mol$_{Fe}$ K^2). With both γ and χ_0 values estimated above the $T_2=26.4$ K transition, the Wilson ratio associated with this high-temperature ordered state is $R\approx 2$, a value expected for strongly correlated electron systems.

The low-temperature dependence of the resistivity [Fig. 3(b)] reveals metal-like behavior with a residual resistivity $\rho_0\approx 45$ $\mu\Omega$ cm. This is notably different from the resistivity reported by Todorov *et al.*:[7] even though their susceptibility data reveal two phase transitions around the same temperatures as in our measurements, both transitions are absent in their resistivity data for current along the b axis. We have also measured nearly linear resistivity down to 2 K on poor quality crystals, which were hollow rods with flux inclusions. All measurements shown in the current study were performed on high quality crystals, which were confirmed to be well-formed full rods. By plotting $\Delta\rho$ vs T^2 [Fig. 3(d)], where $\Delta\rho(T)=\rho(T)-\rho_0=AT^2$, a clear Fermi-liquid regime is observed below $T\approx 15$ K for both $H=0$ (crosses) and $H=9$ T (triangles). The coefficient A of the quadratic resistivity term is determined to be $A=0.25$ $\mu\Omega$ cm K^{-2}, remarkably large and field independent. When normalizing A by the low-temperature quasiparticle effective mass $\gamma=0.02$ J/(mol$_{Fe}$ K^2), the KW ratio A/γ^2 is almost two orders

of magnitude larger than for heavy fermion materials: $A/\gamma^2 = 55a_0$, where $a_0 = 10^{-5}$ $\mu\Omega$ cm mol^2 K^2 mJ^{-2} is a nearly universal value observed in strongly correlated electron systems.[21] This value is among the largest KW ratios reported (Fig. 5), significantly smaller only than that of Sr_2RuO_4 for current normal to the RuO_2 planes.[22] Various mechanisms have been proposed to explain the large KW ratios. Magnetic frustration or the proximity to a quantum critical point (QCP) was considered likely scenarios for the $A/\gamma^2 = 60a_0$ observed in $Na_{0.07}CoO_2$.[23] In Sr_2RuO_4, the KW ratio was highly anisotropic, likely due to the two-dimensional character of the Fermi liquid, and the reduced dimensionality may be the cause for enhanced KW ratio in $Cu_{0.07}TiSe_2$.[24] The fact that A and γ are nearly field independent up to 9 T in $CaFe_4As_3$ does not immediately justify a "QCP" scenario, although it will be important to study the effect of pressure or doping on the possible SDW state and the low-temperature transition. The reduced dimensionality of the Fermi liquid cannot explain the high KW ratio either, given the three-dimensional (3D) character of the structure in $CaFe_4As_3$. Modest magnetic frustration may be present in this compound given that the Weiss temperatures θ_b and θ_{ac} are ~ -220 and -150 K, respectively, 2 to 2.5 times larger than $T_N = 88.0$ K. It will be necessary to study the microscopic magnetic structure to determine whether the Fe sublattice is indeed frustrated, and this work is currently underway.

In conclusion, $CaFe_4As_3$ displays a Fermi-liquid behavior at low temperatures, with enhanced electron-electron correlations as indicated by the value of the electronic specific heat coefficient $\gamma = 0.02$ J/(mol$_{Fe}$ K^2) and an unusually high KW ratio $A/\gamma^2 = 55a_0$. A low-temperature transition exists in this compound around $T_2 = (26.4 \pm 1.0)$ K, marked by a remarkably sharp resistivity drop and abrupt increase in susceptibility. Experiments involving low-temperature neutron diffraction are underway to elucidate the nature of the magnetic structure below and above this transition and to clarify whether it is magnetic in nature or it has a structural component as well. At higher temperatures, AFM order occurs below $T_N = (88.0 \pm 1.0)$ K, which is likely associated with a SDW state as suggested by the small increase in the resistivity below T_N. Although not superconducting and with a more 3D crystal structure than the iron pnictides, $CaFe_4As_3$ resembles the "1-2-2" superconductors with regards to the high-temperature SDW ordering, the enhanced electron mass γ, and also the Fe-As sheets. Together with the enhanced R and KW ratios, the room-temperature resistivity values around 0.3 m Ω cm, comparable to those of LaFeOP (Ref. 1) and AFe_2As_2 [A=Ba (Ref. 14) or Ca (Ref. 17)], qualify $CaFe_4As_3$ as a metal with enhanced electron correlations.

We would like to thank Q. Si, D. Natelson, and M. Dzero for useful discussions. E.M. acknowledges support from Rice University. Work at U.C. Davis was funded by NSF (Grant No. DMR-0600742).

[1] Y. Kamihara, T. Watanabe, M. Hirano, and H. Hosono, J. Am. Chem. Soc. **130**, 3296 (2008).
[2] P. L. Alireza, Y. T. C. Ko, J. Gillett, C. M. Petrone, J. M. Cole, G. G. Lonzarich, and S. E. Sebastian, J. Phys.: Condens. Matter **21**, 012208 (2009).
[3] M. Rotter, M. Tegel, and D. Johrendt, Phys. Rev. Lett. **101**, 107006 (2008).
[4] F. C. Hsu, J. Y. Luo, K. W. Yeh, T. K. Chen, T. W. Huang, P. M. Wu, Y. C. Lee, Y. L. Huang, Y. Y. Chu, D. C. Yan, and M. K. Wu, Proc. Natl. Acad. Sci. U.S.A. **105**, 14262 (2008).
[5] J. H. Tapp, Z. Tang, B. Lv, K. Sasmal, B. Lorenz, P. C. W. Chu, and A. M. Guloy, Phys. Rev. B **78**, 060505(R) (2008).
[6] C. W. Chu, F. Chen, M. Gooch, A. M. Guloy, B. Lorenz, B. Lv, K. Sasmal, Z. J. Tang, J. H. Tapp, and Y. Y. Xue, Physica C **469**, 326 (2009).
[7] I. Todorov, D. Y. Chung, C. D. Malliakas, Q. Li, T. Bakas, A. Douvalis, G. Trimarchi, K. Gray, J. F. Mitchell, A. J. Freeman, and M. G. Kanatzidis, J. Am. Chem. Soc. **131**, 5405 (2009).
[8] G. M. Sheldrick, Acta Crystallogr. **A64**, 112 (2008); ; *Bruker SMART, v. 5.054* (Bruker AXS Inc., Madison, Wisconsin, 2002); *SAINT, v. 7.46a* (Bruker AXS Inc., Madison, Wisconsin, 2007).
[9] See EPAPS Document No. E-PRBMDO-80-R16926 for tables of crystallographic data. For more information on EPAPS, see http://www.aip.org/pubservs/epaps.html.
[10] R. L. Carlin, *Magnetochemistry* (Springer, New York, 1986).
[11] N. W. Ashcroft and N. D. Mermin, *Solid State Physics*, (Harcourt College Publishing, New York, 1976).
[12] C. de la Cruz, Q. Huang, J. W. Lynn, J. Li, W. R. II, J. L. Zarestky, H. A. Mook, G. F. Chen, J. L. Luo, N. L. Wang, and P. Dai, Nature (London) **453**, 899 (2008).
[13] Q. Huang, Y. Qiu, W. Bao, M. A. Green, J. W. Lynn, Y. C. Gasparovic, T. Wu, G. Wu, and X. H. Chen, Phys. Rev. Lett. **101**, 257003 (2008).
[14] N. Ni, S. L. Bud'ko, A. Kreyssig, S. Nandi, G. E. Rustan, A. I. Goldman, S. Gupta, J. D. Corbett, A. Kracher, and P. C. Canfield, Phys. Rev. B **78**, 014507 (2008).
[15] E. Fawcett, Rev. Mod. Phys. **60**, 209 (1988).
[16] J. Dong, H. J. Zhang, G. Xu, Z. Li, G. Li, W. Z. Hu, D. Wu, G. F. Chen, X. Dai, J. L. Luo, Z. Fang, and N. L. Wang, EPL **83**, 27006 (2008).
[17] N. Ni, S. Nandi, A. Kreyssig, A. I. Goldman, E. D. Mun, S. L. Bud'ko, and P. C. Canfield, Phys. Rev. B **78**, 014523 (2008).
[18] K. G. Wilson, Rev. Mod. Phys. **47**, 773 (1975).
[19] K. Yamada, Prog. Theor. Phys. **53**, 970 (1975).
[20] S. R. Julian, A. P. Mackenzie, G. G. Lonzarich, C. Bergemann, R. K. W. Haselwimmer, Y. Maeno, S. NishiZaki, A. W. Tyler, S. Ikeda, and T. Fujita, Physica B **259-261**, 928 (1999).
[21] N. Tsujii, K. Yoshimura, and K. Kosuge, J. Phys.: Condens. Matter **15**, 1993 (2003).
[22] Y. Maeno, K. Yoshida, H. Hashimoto, S. Nishizaki, S. ichi Ikeda, M. Nohara, T. Fujita, A. P. Mackenzie, N. E. Hussey, J. G. Bednorz, and F. Lichtenberg, J. Phys. Soc. Jpn. **66**, 1405 (1997).
[23] S. Y. Li, L. Taillefer, D. G. Hawthorn, M. A. Tanatar, J. Paglione, M. Sutherland, R. W. Hill, C. H. Wang, and X. H. Chen, Phys. Rev. Lett. **93**, 056401 (2004).
[24] E. Morosan, L. Li, N. P. Ong, and R. J. Cava, Phys. Rev. B **75**, 104505 (2007).